Description and validation of a dynamic tool for the modelling of a solar-assisted absorption cooling machine

Gianpiero Evola[1*], Nolwenn Le Pierrès[1], François Boudehenn[2], Philippe Papillon[2]

[1] LOCIE, CNRS FRE3220 - Université de Savoie, Polytech'Annecy-Chambery, Savoie Technolac, 73376 Le Bourget-Du-Lac Cedex, France.

[2] INES, CEA-LITEN, BP332, 73377 Le Bourget-Du-Lac Cedex, France

[*] Corresponding Author, gianpiero.evola@univ-savoie.fr

Abstract

In recent years, the electricity consumption due to buildings air-conditioning has relevantly increased. As an alternative to conventional air-conditioning systems, solar cooling processes can satisfactorily meet the cooling load and the comfort demand at a very low energy cost.

In the context of the French research project ORASOL, a small-size solar-assisted cooling system based on a water-cooled H_20-LiBr absorption machine is being tested at INES (Institut National de l'Energie Solaire). The absorption machine is distributed by Rotartica, with a nominal cooling power as high as 4.5 kW, powered by 30 m^2 flat plate solar collectors. The heat rejection is carried out through a horizontal ground heat exchanger. The installation has been built in the framework of the European project SOLERA (www.solera-project.eu), coordinated by Fraunhaufer ISE.

In this paper the analytical model for the dynamic simulation of the entire system is presented. Special attention is paid to the simulation of the storage tank, by accounting for thermal stratification, and the flat-plate solar collectors, which are modelled by means of a slightly simplified but very reliable approach. The experimental results, collected during summer 2009, are used for the validation of the models, both for the components and the whole installation.

1. Introduction

A simplified scheme of the test facility installed at INES is reported in Fig. 1. The absorption chiller has a nominal cooling capacity as high as 4.5 kW, measured at the following conditions:

- Water inlet temperature at generator: 90°C.
- Water outlet temperature at evaporator: 12°C.
- Cooling water inlet temperature: 30°C.

The chiller is powered by hot water produced through a solar section composed of 25 flat-plate solar collectors (30 m^2 overall net absorbing surface); the collectors are installed on the roof of the building with a 30° tilt angle and facing south, and they are arranged in two batteries put in series. Actually, the collector field is slightly oversized with respect to the thermal power required by the absorption machine for summer operation, as it also accounts for winter heating. A compact heat exchanger separates the solar section from a four hundred-litre hot water tank. The latter is placed inside the building, and the pipes between the collectors and the tank are very well insulated. An electric

resistance is also available as a back-up system on the storage, but it was not used as the aim of the project was to investigate the performance of the system when powered only by solar energy. The chiller is water-cooled, and heat rejection is assisted by a ground heat exchanger made up with twenty-two horizontal polyethylene pipes divided into two layers, buried at a depth of 0.7 m and 1.1 m, respectively; the length of each pipe is around 100 m. On the user side, the cold water produced by the absorption machine is stored in a water tank, and then distributed to fan-coils for the air-conditioning of some offices. Anyway, in this paper attention will not be paid to the cold water storage and distribution; the aim is the description and the validation of the models of all the components of the solar section, as well as their coupling to the model already developed for the absorption machine, by taking into account the control logic implemented on the test facility.

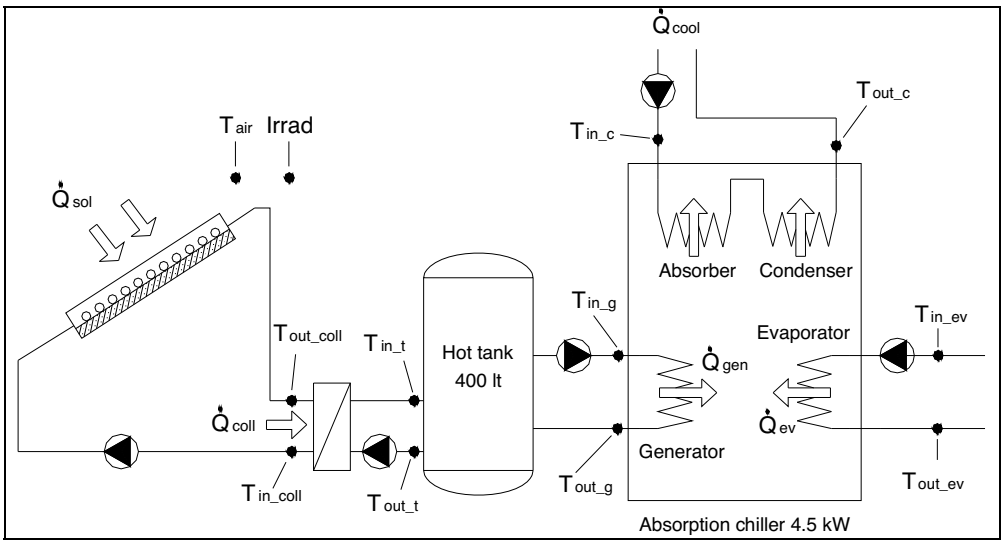

Fig. 1. Simplified scheme of the experimental facility.

Fig. 1 also reports the position of the main measurement devices. All the temperatures at the inlet and outlet of each component are registered, as well as the outdoor temperature and the solar irradiation available on the collectors surface. A value is provided for each parameter every 120 seconds, as an average of the measurements within the last acquisition period. No measurements are available for the internal parameters of the absorption machine (pressures, temperatures, salt concentrations).

2. Modelling of the solar field

2.1. Description of the model

The simulation of the performances of solar collectors is often carried out by means of over-simplified models, based on the definition of collector efficiencies. Such models are very simple to implement and require very few parameters for the characterization of the component, which are normally provided by the manufacturers. However, the precision of the results is not always good, and the thermal inertia of the absorber plate can not be taken into account. On the contrary, very detailed models are available in the literature, based on an accurate description of the physical phenomena occurring in solar collectors; despite their precision, such models need a high number of parameters as

an input, most of which are not easily known and can only be roughly assessed, so introducing a certain degree of uncertainty in the results.

In this work, an intermediate approach is chosen. The energy balance on the collector is written as in Eqn. (1), and it accounts for the thermal inertia of the absorber plate and for the "fin effect" in the thermal exchange between absorber and tubes (F, fin efficiency), as described in [1]. Such an equation refers to a control volume represented by a single pipe and the section of absorber on which it is welded, as shown in Fig. 2.

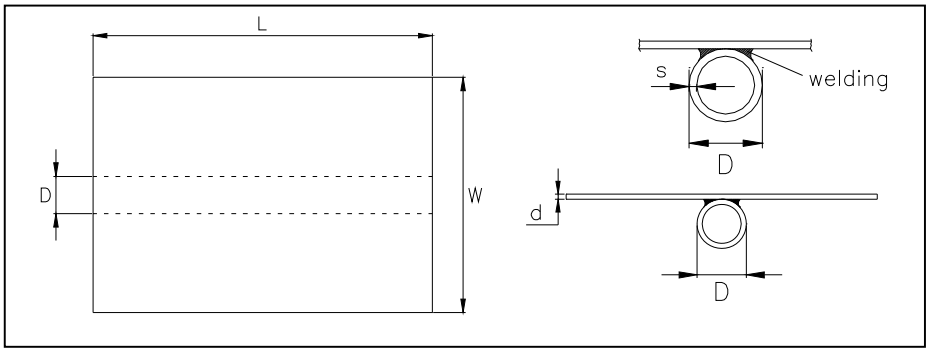

Fig. 2. Size of an element of the absorber plate.

$$\left[(W-D)\cdot F+D\right]\cdot L\cdot\left[I_{sol}\cdot(\tau\alpha)_{\theta}-U_L\cdot(T_p-T_{air})\right]-\dot{Q}_w=M\cdot c_p\cdot\frac{dT_p}{dt} \qquad (1)$$

Actually, a flat-plate solar collector is made up of a number *n* of such elements, arranged in parallel, hence the fluid outlet conditions can be assessed by studying a single element. The model also accounts for the effect of the incidence angle θ of the sunbeams on the glass cover. The *fin efficiency* introduced in Eqn. (1) is defined as in Eqn. (2), and it accounts for the actual temperature distribution on the absorber plate, as in Eqn. (1) an uniform temperature T_p is considered.

$$F=\tanh\left(m\cdot\frac{W-D}{2}\right)\Big/\left(m\cdot\frac{W-D}{2}\right) \qquad \text{where:} \qquad m=\sqrt{\frac{U_L}{\lambda\cdot d}} \qquad (2)$$

In order to apply such a model, the only data needed to characterize the component are the size of the absorber plate (W × L × d) and its weight (M), the external pipe diameter (D), as well as the overall loss coefficient (U_L) and the effective transmittance-absorptance product (τα), which may be easily known from the manufacturer,. Furthermore, the absorber thermal conductivity λ and thermal capacity c_p must be taken into account. The model is completed by Eqn. (3), which provides the thermal power delivered to the fluid, and Eqn. (4), which links fluid and absorber temperatures by accounting for the heat transfer between them.

$$\dot{Q}_w=\dot{m}\cdot c_{pf}\cdot\left(T_{out}-T_{in}\right) \qquad (3)$$

$$T_{out}=T_p+(T_{in}-T_p)\cdot e^{-\frac{UA}{\dot{m}\cdot c_{pf}}} \qquad (4)$$

2.2. Parameters identification

Most of the parameters introduced in Eqn. (1) to (4) can be easily determined from the technical documents provided by the manufacturer. In the experimental facility installed at INES the flat-plate collectors TGD th Y2.4 distributed by CLIPSOL are used, whose features are reported in Table 1.

Table 1. Main parameters for the CLIPSOL TGD th Y2.4 collectors

W [m]	D [m]	L [m]	d [m]	s [m]	M [kg]	η_0 [-]	a_1 [-]
0.125	0.008	2.4	0.0005	0.0015	0.77	0.73	3.74

As far as the fluid is concerned, it is to remind that in the experimental facility a mixture of water (80%) and glycolic ethylene (20%) is used, whose specific thermal capacity c_{pf} can be assessed as a function of the temperature according to [2]. The fluid flow rate is known: when the pump on the primary circuit is switched on, an overall flow rate as high as 1.27 m^3/h is measured by the flow meters installed on the experimental facility. This overall flow rate is then distributed into the collectors: we can count 48 and 52 pipes in the first and the second series of collectors, respectively. In Eqn. (4) the overall thermal transmittance UA between fluid and absorber is used; its value can be assessed as:

$$UA = \left[\frac{1}{h_i \cdot \pi \cdot (D - 2 \cdot s) \cdot L} + \frac{R_s}{L} \right]^{-1} \tag{5}$$

Here h_i = 1500 $W \cdot m^{-2} \cdot K^{-1}$ is the internal convective coefficient, calculated through well-known relations for forced convection into cylindrical ducts, whereas R_s is the thermal resistance of the welding. According to [1], a good welding should not introduce a thermal resistance higher than 0.03 $W \cdot m^{-1} \cdot K^{-1}$; in case of well-done welding, we can assume $R_s = 0.01 W \cdot m^{-1} \cdot K^{-1}$.

The effective transmittance-absorptance product for normal incidence $(\tau\alpha)_n$ can be assessed through Eqn. (6), where $\alpha_n = 0.95$ for a black-painted selective absorber, $\rho_d = 0.15$ for the reflection of the diffuse radiation on the glass and $\tau_n = 0.9$ for a 3-mm thick low iron-oxide glass. The model adopted in this study also accounts for the variation of $(\tau\alpha)$ with the incidence angle of the sunbeams, according to the correction coefficient provided by Klein [1].

$$(\tau\alpha)_n = \frac{\tau_n \cdot \alpha_n}{1 - (1 - \alpha_n) \cdot \rho_d} = 0.86 \tag{6}$$

Finally, the overall loss coefficient U_L can be determined from the knowledge of the characteristic equation of the collector. The intersection η_0 and the slope a_1 of the efficiency curve for the CLIPSOL TGD th Y2.4 are reported in Table 1; the relation for the calculation of U_L is the following:

$$U_L = \frac{a_1}{\eta_0} \cdot (\tau\alpha)_n = 4.4 \qquad [W \cdot m^{-2} \cdot K^{-1}] \tag{7}$$

2.3. Validation of the model

In order to evaluate the reliability of the model, the equations previously described have been implemented on the simulation tool SimSPARK, and the experimental results collected on a sample day (14th August 2009) have been compared to the output provided by the software. The input data necessary for the simulation are the outdoor air temperature, the solar irradiation on the collector surface (see Fig. 3) and the fluid temperature at the outlet of the heat exchanger (T_{in_coll}, see Fig. 1). As an output, the model calculates the fluid temperature at the inlet of the heat exchanger (T_{out_coll}, see Fig. 1) and the overall thermal power collected by the collector field.

As described before, the model is able to account for the variation of the optical properties of glass and absorber with the incidence angle θ of the sunbeams. In order to exploit such a feature, the equations for the calculation of the incidence angle as a function of time, collector tilt angle (β = 30°) and latitude (φ = 45.5°) [1] were also implemented. The results of the validation are reported in Fig. 4; the prediction of the outlet temperature is very satisfactory, as the error during operation time (9:00 – 17:30) is always lower than 0.5°C. The thermal power collected by the solar field is also predicted very well, with a daily average error on the overall daily energy as high as 2.1%. When water is not flowing through the collectors, its temperature at the solar field outlet may not be assessed by means of the previous model and a higher degree of error might occur.

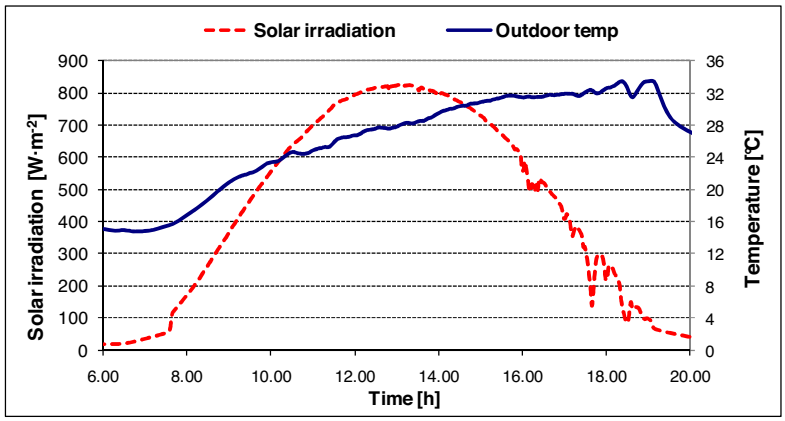

Fig. 3. Daily solar irradiation and outdoor temperature profile (14th August 2009)

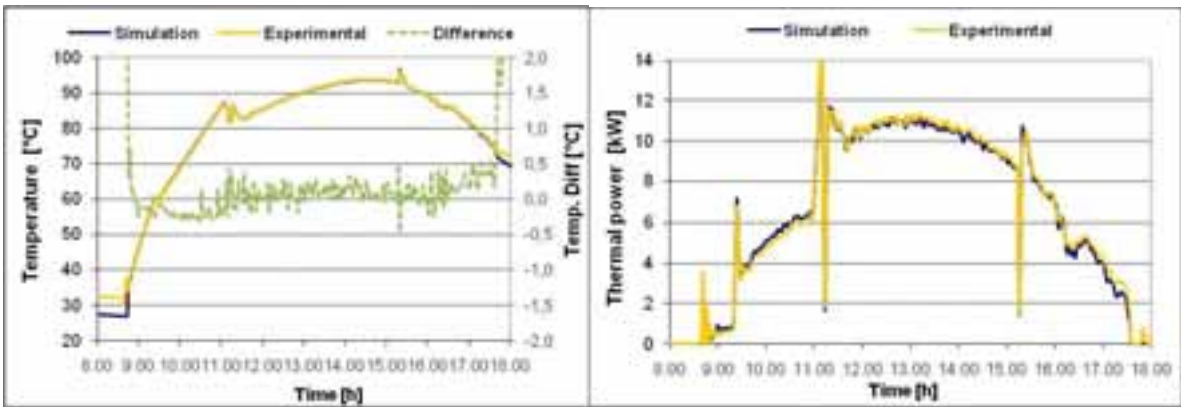

Fig. 4. Comparison between experimental and simulated output

3. Modelling of the other components

3.1. Storage tank

The model for the simulation of the thermally stratified storage tank is inspiredfrom the one presented by Bourdoukan et al. [3]. However, such a model has been modified in order to account for the actual position of the water inlet and outlet on the tank (see Fig. 5). The storage tank is divided into n = 12 layers; the hot water from and to the solar section is exchanged in the central part of the storage (fifth and ninth layer), whereas the water from and to the generator of the absorption machine is exchanged in the outermost layers.

The general structure of the energy balance on one layer is shown in Eqn. (8), where the heat fluxes due to the mass transfer and to the conduction process are accounted for, as well as the thermal losses through the envelope. When the absorption chiller is not working ($m_{gen} = 0$), but the tank is still being charged from the solar side ($m_{tank} \neq 0$), the outer layers (from 1 to x-1 and from y+1 to n) would not be involved. In order to account for the internal circulation induced by natural convection, two additional internal flow rates have been introduced, as half the main flow rate ($m_{sup} = m_{inf} = 0.5 \cdot m_{tank}$). An example of the energy balance on such outer layers is reported in Eqn. (9).

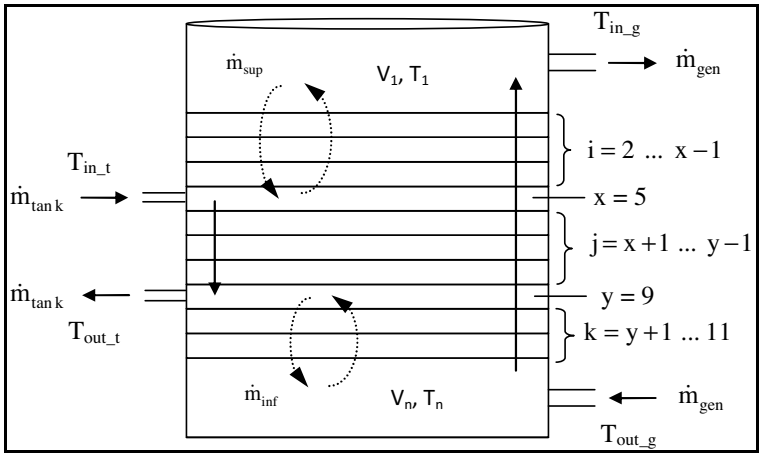

Fig. 5. Description of the storage tank

$$M_j c_p \frac{dT_j}{dt} = US_{e,j}\left(T_e - T_j\right) + \dot{m}_{gen} c_p \left(T_{j+1} - T_j\right) + \dot{m}_{tank} c_p \left(T_j - T_{j-1}\right) + \frac{\lambda \cdot S}{e_{j-1,j}}\left(T_j - T_{j-1}\right) + \frac{\lambda \cdot S}{e_{j,j+1}}\left(T_{j+1} - T_j\right) \quad (8)$$

$$M_i c_p \frac{dT_i}{dt} = US_{e,i}\left(T_e - T_i\right) + \dot{m}_{gen} c_p \left(T_{i+1} - T_i\right) + \dot{m}_{sup} c_p \left(T_{i+1} - 2T_i + T_{i-1}\right) + \frac{\lambda \cdot S}{e_{i-1,i}}\left(T_i - T_{i-1}\right) + \frac{\lambda \cdot S}{e_{i,i+1}}\left(T_{i+1} - T_i\right) \quad (9)$$

In the previous equations λ and c_p are the water thermal conductivity and thermal capacity, S is the storage section, $S_{e,j}$ the external surface of each layer, $e_{j,j+1}$ the thickness between two consecutive layers; such parameters can be easily calculated starting from the storage dimensions, which are reported in Table 3. Furthermore, T_e is the temperature of the room where the tank is installed. When the absorption machine is switched on, the flow rate delivered to the generator is $m_{gen} = 0.82$ m^3/h; more details about m_{tank} will be provided in the following.

Table 2. Main parameters for the storage tank

Diameter [m]	Height [m]	Mass M [kg]	U [$Wm^{-2}K^{-1}$]
0.53	1.8	400	4.5

For the sake of brevity, the validation of the model of the only storage tank is not shown, as in the following section the model for the simulation of the whole system will be validated.

3.2. Heat exchanger and absorption machine

The heat exchanger installed between the solar field and the storage tank is a compact plate heat exchanger. From the analysis of the experimental data, it is characterised by an efficiency $\eta_{exch} = 0.78$. The knowledge of the efficiency and the fluid mass flow rates, as well as the fluid inlet temperatures, is sufficient to determine the outlet temperatures $T_{in,coll}$ and $T_{in,t}$. The dynamic model of the absorption machine has been described and validated in [4].

4. Coupling of the components and validation

After having tested the models developed for the single components, they have been coupled in order to simulate the behaviour of the whole system. The main aim of the complete model is to foresee the performance of the absorption machine, i.e. the cooling power delivered to the user and its thermal COP; the thermal power required at the generator and rejected through the cooling circuit will also be looked at. On the contrary, in this work we will not draw attention on the intermediate results (fluid temperatures in the solar circuit and in the tank). The input data required by the simulation are the weather data (outdoor air temperature, solar irradiation) and the inlet fluid temperatures at absorber and evaporator, as well as the corresponding flow rates ($m_{cool} = 2.20$ m^3/h, $m_{evap} = 1.34$ m^3/h).
In the model developed on SimSPARK a control logic which regulates the system has also been implemented (see Fig. 1 for the definition of the temperatures):

- The pump on the primary solar circuit starts when the solar irradiation gets higher than 300 $W \cdot m^{-2}$, and stops when it gets lower than 200 $W \cdot m^{-2}$.
- The pump between the exchanger and storage tank starts if $T_{out\_coll} \geq T_{out\_t} + 5°C$; it stops when $T_{out\_coll} \leq T_{out\_t}$.
- The water flow rate delivered to the tank during operation is not constant, as it changes as a function of the temperature in the tank in order to enhance stratification; Fig. 6 reports the flow rate profile during the same day described by now.
- The absorption machine starts when the hot water available in the storage is hot enough ($T_{out\_coll} \geq 80°C$); the machine is turned off when $T_{out\_coll} \leq 76°C$.

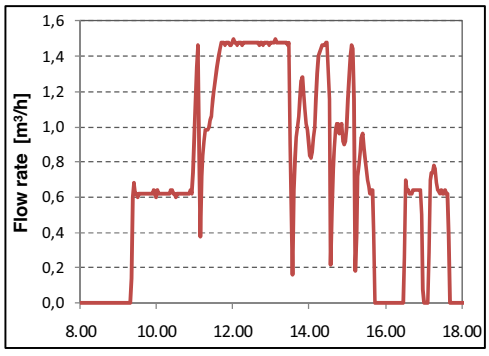

Fig. 6. Flow rate delivered to the storage tank

The experimental results, collected during three sample days in the summer 2009, will be used to validate the overall model resulting from the coupling of the components; the results of the validation are shown in Fig.7.

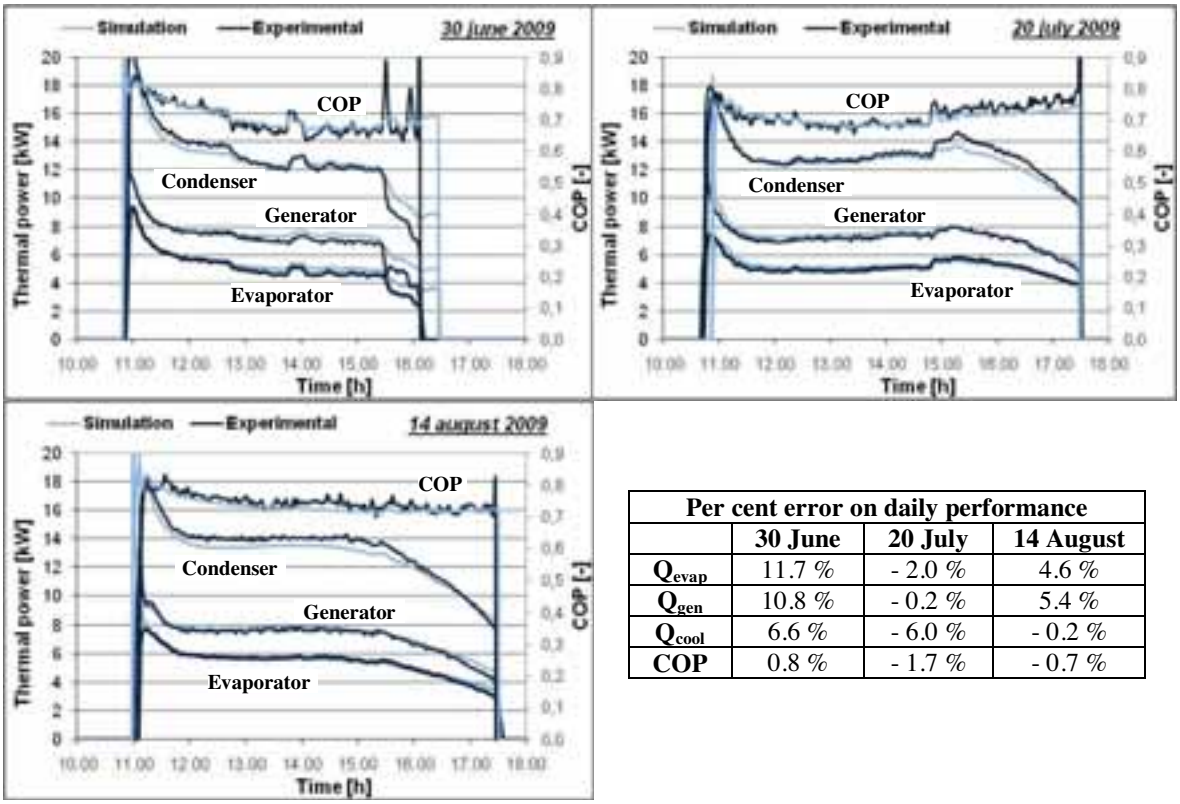

Per cent error on daily performance			
	30 June	**20 July**	**14 August**
Q_{evap}	11.7 %	- 2.0 %	4.6 %
Q_{gen}	10.8 %	- 0.2 %	5.4 %
Q_{cool}	6.6 %	- 6.0 %	- 0.2 %
COP	0.8 %	- 1.7 %	- 0.7 %

Fig. 7. Comparison between simulation and experimental results.

5. Conclusion

The model developed for the simulation of the solar-assisted low-capacity absorption chiller has a good reliability. Fig. 7 shows that the error on the daily performance is usually quite low, and in one case it comes to about 11 %, but the average thermal COP is always well identified. In some cases, a slight time delay or time lead between real and simulated starting/stop of the chiller occurs, which is probably due to some imprecision in the determination of the temperature distribution inside the tank. As expected, the error in the overall model is higher than the one affecting the single components, as reported in [4] for the absorption chiller and in the previous pages for the solar field. However, the model can be regarded as a good and reliable tool to carry out the evaluation of the average performance of the system, even on a long time period.

References

[1] J.A. Duffie, W.A. Beckman, (2006). Solar Engineering of Thermal Processes, John Wiley & S., New Jersey.

[2] K. Ng, A. Rosenberg, M. Bastos, I. Wadso, Heat capacity of poly(ethylene glycol)-water mixtures: Poly(ethylene glycol)-water interactions, Thermochimica Acta, 169 (1990) 339-346.

[3] P. Bourdoukan, E. Wurtz, P. Joubert, M. Spèrandio, Potential of solar heat pipe vacuum collectors in the desiccant cooling process: modelling and experimental results, Solar Energy, 82 (2008) 1209-1219.

[4] G. Evola, N. Le Pierrés, F. Boudehenn, P. Papillon (2010). Simulation and Experimental Results of a Small-size Solar-assisted Absorption Cooling System, Proceedings of ECOS International Conference, Lausanne.